Chemistry and Ecology, 2013
Vol. 29, No. 5, 476–488, http://dx.doi.org/10.1080/02757540.2013.769968

Taylor & Francis
Taylor & Francis Group

An interval dynamic multimedia fugacity (IDMF) model for environmental fate of PAHs and their source apportionment in a typical oilfield, China

Yan Hu, Jingya Wen, Dazhou Wang, Xianyuan Du, and Yu Li*

MOE Key Laboratory of Regional Energy Systems Optimization; Resources and Environmental Research Academy, North China Electric Power University, Beijing, China

(*Received 4 May 2012; final version received 22 January 2013*)

An interval dynamic multimedia fugacity (IDMF) model with a new validation criterion of interval average logarithmic residual error (IALRE) was developed in this study. The environmental fate of polycyclic aromatic hydrocarbons (PAHs) and their source apportionment in a typical oilfield of China were simulated from 1985 to 2010. The PAH concentrations predicted by the model were in agreement with the measured concentrations, which were indicated by the IALREs calculated at 0.41, 0.63, 0.52, and 0.58 for air, water, soil, and sediment, respectively. The multimedia concentrations of Σ16 PAHs were 29.55, 39.22, 31.98, and 26.69 times greater in 2010 than those in 1985, and were higher than any other year modelled. Additionally, 87.82% of PAHs remained in the soil in 2010. PAH source emission into the soil was the major modelled source, whereas PAH degradation in the air was the major modelled loss pathway; the dominant transfer process between the adjacent compartments was atmospheric deposition from air to soil. It was demonstrated that high-temperature combustion was the major source of PAHs in the air and soil, whereas biomass and coal combustion were attributed to water and sediment compartments. The IDMF model was effective in the dynamic source apportionment of PAHs.

Keywords: polycyclic aromatic hydrocarbons; fate; source apportionment; interval; multimedia fugacity model; dynamic

1. Introduction

Polycyclic aromatic hydrocarbons (PAHs) pose substantial concerns owing to their widely known potential toxicity, including mutagenicity, teratogenicity, and carcinogenicity [1]. Pyrogenic and petrogenic sources are two major sources of anthropogenic PAHs in the environment [2]. Pyrogenic PAHs are formed as trace contaminants by the incomplete combustion of organic matter, such as wood, fossil fuels, asphalt, and industrial waste. Crude and refined petroleum both contain petrogenic PAHs and are important sources of PAHs [3]. Petroleum and gas resources are so abundant in China that the total petroleum availability was approximately 186 million tons in 2007, of which nearly 84% was onshore petroleum [4,5]. The large-scale exploitation produces many environmental problems, and once released, PAHs are widely dispersed into the multimedia environment and transferred between different compartments.

*Corresponding author. Email: liyuxx8@hotmail.com

Experimental studies have revealed that significant negative environmental effects of PAHs appear in multimedia environments and cannot be ignored [6]. However, long-term continuous sampling in different compartments is unfeasible because of the high cost and the investment of human resources. In contrast, chemical concentrations in different compartments could be calculated with good agreement by multimedia models. The level III and level IV fugacity models are used under steady-state and unsteady-state assumptions, respectively [7]. Level IV multimedia fugacity models are distribution based models incorporating all environmental compartments and fluxes of pollutants across compartment interfaces, and are appropriate for simulating the time-dependent fate of persistent organic pollutants (POPs) [8]. Uncertainties result from the lack of sufficient information related to model assumption, parameters acquirement, model validation data, etc., which limit the understanding about the pollutants' environmental behaviour. Thus, the modelling of pollutants' environmental fate is inherently linked together with uncertainties.

The traditional method of model uncertainty analysis is the Monte Carlo simulation (MCS), which is on basis of the assumption of distribution functions. Traditional MCS would be a better method to describe model outcome when (1) high-quality data are available on the distributions of modelling input parameters and validation samples; or (2) the multimedia concentrations of the modelling results as a tool for risk assessment will be used as the input of the next risk assessment processes. And inappropriate decisions can be made when the uncertainty in the modelling processes is not effectively treated. In contrast, interval arithmetic [9,10] could express the range of parameters regardless of the distribution function and all the possible values are contained in the interval solutions. Moreover, the chemical concentration always varies in a wide range owing to the heterogeneity of the environmental system, and the validation with an interval solution could well embody the consistency between the modelled values and the measured ones.

Various methods are being applied in PAHs source identification and apportionment. Diagnostic ratios (DR) of PAHs have been widely used to characterise and identify emission sources in various environments owing to the flexibility of application [11,12]. Yunker performed an assessment of PAHs source composition in the Fraser River Basin, establishing PAHs sources [13]. Morillo et al. [14] also determined PAH sources using diagnostic PAH ratios. To aid in interpreting dynamic multimedia source apportionment, diagnostic ratios of PAHs in the multimedia environments can also be calculated from the dynamic multimedia fugacity model outputs.

In this paper, an interval dynamic multimedia fugacity (IDMF) model and a new validation criterion are first described, and they are applied to investigate the dynamic multimedia environmental fate of 16 PAHs and their source apportionment in a typical petroleum exploration region in China between 1985 and 2010. The model is an extension of the level IV fugacity model of Mackay [15] using the interval analysis arithmetic. When applied to the contaminated environmental system, the model could be used to guide management decisions and risk assessment.

2. Materials and methods

2.1. *Study area description*

The study area has a population of 2.73 million and total area of 21,219 km^2, and a continental monsoon climate. The seasonal mean temperatures range from -22.6°C in December to 36.5°C in June with a mean annual temperature of 3.3°C. The annual precipitation is approximately 314.1 mm, and the evaporation is 1257.5 mm. The average and fastest wind speeds are 2.5 ms^{-1} and 12.3 ms^{-1}, respectively [16]. The oil resources are very abundant, and more than 40 million tons of petroleum has been exploited for decades from the thousands of oil wells in this area, with most of them operating continuously.

2.2. *Interval dynamic multimedia fugacity model*

The fugacity approach has been shown to be effective at describing the multimedia behaviour of organic chemicals in a variety of environments, described in detail by Mackay [15]. The non-steady-state mass balance is described with the following system of linear differential equations:

$$\frac{\mathrm{d}f_i}{\mathrm{d}t} = \frac{\left[E_i + G_{Ai}c_{Bi} + \sum D_{ji}f_j - \left(\sum D_{ij} + D_{Ri} + D_{Ai}\right)f_i\right]}{V_i Z_i} \tag{1}$$

V_i is the volume of compartment i (m^3); Z_i is the fugacity capacity of compartment i ($mol \cdot m^{-3} \cdot Pa^{-1}$); f_i is the fugacity of compartment i (Pa); E_i is the emission rate into compartment i ($mol\,h^{-1}$); G_{Ai} is the advection inflow rate of compartment i ($m^3\,h^{-1}$); c_{Bi} is the inflow concentration of the adjacent region to compartment i ($mol\,m^{-3}$); D_{ij} is the transfer rate coefficient from compartment i to j ($mol\,Pa^{-1}\,h^{-1}$); and D_{Ai} and D_{Ri} represent the advection outflow rate coefficient and degradation rate coefficient of compartment i ($mol\,Pa^{-1}\,h^{-1}$), respectively.

High model uncertainty is typically introduced by a combination of model assumptions, parameter uncertainty, and complexity of the multimedia environmental system. The uncertainty information in the model can be described in the model equations. Thus, the mathematical expression of interval arithmetic [9] is used to better describe the model equations.

Briefly, parameter x in the model is rewritten as $x^{\pm}$ so that:

$$x^{\pm} = [x^-,\ x^+] = \{x^- \le x \le x^+\} \tag{2}$$

In Equation (2), x^+ and x^- represent the upper bound and lower bound, respectively, of interval value $x^{\pm}$, and $x^{\pm}$ is a determined value only when $x^{\pm} = x^- = x^+$.

According to the method of interval arithmetic, an IDMF model is developed based on the determined fugacity model (1), which could be adapted as follows:

$$\left(\frac{\mathrm{d}f_i}{\mathrm{d}t}\right)^{\pm} = \frac{\left[E_i^{\pm} + G_{Ai}^{\pm}c_{Bi}^{\pm} + \sum D_{ji}^{\pm}f_j - \left(\sum D_{ij}^{\pm} + D_{Ri}^{\pm} + D_{Ai}^{\pm}\right)f_i\right]}{V_i^{\pm}Z_i^{\pm}} \tag{3}$$

Furthermore, model (3) could be divided into a deterministic upper bound sub-model (4) and a lower bound sub-model (5) on the basis of sensitivity analysis:

$$\left(\frac{\mathrm{d}f_i}{\mathrm{d}t}\right)^{+} = \left[\frac{E_i^{+} + G_{Ai}^{+}c_{Bi}^{+} + \sum D_{ji}^{+}f_j - \left(\sum D_{ij}^{-} + D_{Ri}^{-} + D_{Ai}^{-}\right)f_i}{V_i^{-}Z_i^{-}}\right] \tag{4}$$

$$\left(\frac{\mathrm{d}f_i}{\mathrm{d}t}\right)^{-} = \left[\frac{E_i^{-} + G_{Ai}^{-}c_{Bi}^{-} + \sum D_{ji}^{-}f_j - \left[\sum D_{ij}^{+} + D_{Ri}^{+} + D_{Ai}^{+}\right]f_i}{V_i^{+}Z_i^{+}}\right] \tag{5}$$

The solution of the sub-model should be on the basis of sensitivity analysis so that the characters for each input parameter are distinct. Then, the sub-models of the IDMF model are individually programmed using Matlab software, and the system of first-order differential equations is solved by the Euler method at hourly time steps. The initial fugacity values are set as the environmental background values, and the modelled fugacity values from the previous time step serve as the initial values for the succeeding phase [8]. For each value of t, the values of the fugacities $f_i = f_i(t)$ are multiplied by the fugacity capacity Z_i to determine the value of concentration $C_i = C_i(t)$. The determined solutions of these two sub-models reveal the interval solutions of the IDMF model.

Model validation and sensitivity analysis are important means for evaluating multimedia fugacity models. In the validation of large-scale model, the deviations between the modelled values

and the measured values of less than 1 logarithmic unit indicated good agreement [17]. The logarithmic residual error (LRE) was dimensionless, and was usually used to describe the reliability fof the model [8]. Further, a new validation criterion of interval average logarithmic residual error (IALRE) for the IDMF model was developed to satisfy both the lower and upper bounds, described as:

$$\mathrm{IALRE} = \frac{(\mathrm{LREl} + \mathrm{LREu})}{2} \tag{6}$$

where LREl is the LRE for the lower bound and LREu is the one for the upper bound.

The primary advantages of the developed IDMF model are as follows: (1) the uncertainties information from the modelling parameters can be reflected in the linear differential equations directly, regardless of the distribution function; (2) the measured interval concentrations compared with the modelled interval values is more reliable than the compassion between the measured and modelled average concentrations, for which the measured concentrations in the environment always vary in a relatively large range owing to the internal variability of the environmental system.

A mathematical model was used to determine the relative contribution of each input parameter to the model result. The sensitivity coefficient (S_x) is defined as the ratio of the relative variation of the estimated concentration to that of the input parameter:

$$S_{xi} = \frac{\Delta Y_i / Y_i}{\Delta X_i / X_i} \tag{7}$$

where S_{xi} represents the sensitivity coefficient of input parameter i and X_i and Y_i represent input parameter i and the corresponding modelled concentration [8].

2.3. *Modelling processes and parameters*

A developed IDMF model was applied to simulate the dynamic environmental behaviours of 16 PAHs from 1985 to 2010. Air (pure air and particulates), water (pure water and suspended solids), soil (air, water, and solids), and sediment (water and solids) were the four bulk compartments included in the model. The environmental processes taken into consideration were source emissions in air, water, and soil bulk compartments; advection inflow and outflow in air and water between the study area and the neighbouring area; mass exchanges between inter-compartments; and degradation in the four bulk compartments.

The input parameters to the IDMF model comprised environmental attribute parameters, the physicochemical properties of 16 PAHs, and source emission data. The interval values of the relevant environmental parameters and physicochemical properties for the 16 PAHs are listed in Tables 1 and 2.

The interval values of the major modelling parameters were determined based on the acquirement of the deterministic lower bound and upper bound. For instance, the depth of water compartment was obtained by the interval depth (the minimum and maximum level) of water compartment.

2.4. *Sources estimation*

The emission data for 16 PAHs in air, water, and soil compartments were not always readily available, and the data showed large uncertainty. The amounts of local annual energy consumption and petroleum extraction were used to estimate the emission rates, which were obtained from the statistics yearbooks in the study area from 1985 to 2010. PAH emission sources in the air compartment primarily comprised the following: combustions of biomass (forestry, rice straw, wheat, and corn), coal, coke, natural gas, gasoline, diesel, fuel oil, and liquefied petroleum gas (LPG). The emissions from these sources were calculated by multiplication of the local energy

Table 1. Interval values of characteristic environmental attribute parameters in the study area.

Symbol	Unit	Definition	Interval values
A_a	m^2	Area of air compartment	$[5.1 \times 10^9, 2.12 \times 10^{10}]^a$
h_a	m	Height of air compartment	$[1.00 \times 10^3, 2.00 \times 10^3]^b$
ρ_a	$kg\,m^{-3}$	Density of air compartment	$[1.19 \times 10^0, 1.19 \times 10^0]^c$
rp_a		Density of solids in air	$[1.50 \times 10^3, 1.50 \times 10^3]^c$
A_w	m^2	Area of water compartment	$[1.47 \times 10^8, 2.93 \times 10^9]^a$
h_w	m	Height of water compartment	$[0.67 \times 10^0, 1.80 \times 10^0]^a$
ρ_w	$kg\,m^{-3}$	Density of water compartment	$[1.00 \times 10^3, 1.00 \times 10^3]^b$
rp_w	$kg\,m^{-3}$	Density of solids in water	$[2.40 \times 10^3, 2.40 \times 10^3]^b$
fp_w		Organic carbon content in solids in water	$[4.00 \times 10^{-2}, 4.00 \times 10^{-2}]^b$
A_s	m^2	Area of soil compartment	$[4.95 \times 10^9, 1.83 \times 10^{10}]^a$
h_s	m	Height of soil compartment	$[1.00 \times 10^{-1}, 1.00 \times 10^0]^b$
ρ_s		Density of water compartment	$[1.50 \times 10^2, 2.40 \times 10^2]^b$
V_{ws}		Volume fraction of water in soil	$[3.00 \times 10^{-1}, 3.00 \times 10^{-1}]^b$
rp_s		Density of solids in soil	$[2.40 \times 10^3, 2.40 \times 10^3]^{b,c}$
fp_s		Organic carbon content in solids in soil	$[1.70 \times 10^{-2}, 1.70 \times 10{-}2]^b$
V_{as}		Volume fraction of air in soil	$[2.00 \times 10^{-1}, 2.00 \times 10^{-1}]^b$
A_{sed}	m^2	Area of sediment compartment	$[1.47 \times 10^8, 2.93 \times 10^9]^a$
h_{sed}	m	Height of sediment compartment	$[5.00 \times 10^{-2}, 1.00 \times 10^0]^b$
ρ_{sed}	$kg\,m^{-3}$	Density of sediment compartment	$[1.50 \times 10^2, 2.40 \times 10^2]^{b,c}$
V_{wsed}		Volume fraction of water in sediment	$[7.00 \times 10^{-1}, 7.00 \times 10^{-1}]^b$
rp_{sed}	$kg\,m^{-3}$	Density of solids in sediment	$[2.40 \times 10^3, 2.40 \times 10^3]^{b,c}$
fp_{sed}		Organic carbon content in solids in sediment	$[3.10 \times 10^{-3}, 2.00 \times 10^{-1}]^b$
Q		Scavenging rate	$[2.00 \times 10^5, 2.00 \times 10^5]^b$
U_r	$m\,h^{-1}$	Rain rate	$[9.70 \times 10^{-5}, 9.70 \times 10^{-5}]^b$
U_p	$m\,h^{-1}$	Dry deposition velocity	$[1.10 \times 10^0, 1.10 \times 10^0]^b$
U_{ww}	$m\,h^{-1}$	Water runoff rate from soil	$[1.14 \times 10^{-6}, 1.14 \times 10^{-6}]^b$
U_{sw}	$m\,h^{-1}$	Soil runoff rate from soil	$[2.30 \times 10^{-8}, 2.30 \times 10^{-8}]^b$
U_{dp}	$m\,h^{-1}$	Sediment deposition rate	$[4.60 \times 10^{-8}, 4.60 \times 10^{-8}]^b$
U_{rsed}	$m\,h^{-1}$	Sediment resuspension rate	$[1.10 \times 10^{-8}, 1.10 \times 10^{-8}]^b$

[a]The values were derived from literature [16].
[b]The values were derived from literature [17].
[c]The values were derived from literature [18].

consumption and the corresponding emission factors (EFs) [20]. Source emissions in water and soil compartments were estimated by measuring the annual petroleum extraction volume in the study area because those PAH pollutants from petroleum extraction were the primary input pathways for the oilfield. PAH emissions in the water compartment include the discharge of drilling wastewater and well-flushing wastewater, and the dynamic emission rate for PAHs in the water compartment was estimated by considering oil exploitation amount, PAH content percentage, and the removal rate in oily wastewater [21]. The source emission for the soil compartment was calculated assuming that the ground crude oil amount was 0.5–2.0 tons per oil well per year, and an 85% recovery [22], with the remainder released into soils could be estimated. Interval parameters were applied in the multimedia sources estimation, and the average values for the emission rate in the different compartments are shown in Figure 1. The oscillating pattern for soil and water emission rates in the later simulation years resulted from the fluctuation of the actual petroleum extraction amount in the study area.

3. Results and discussion

3.1. *Parameters sensitivity analysis*

Sixty-two input parameters were included in the IDMF model, which was qualitatively and quantitatively studied using sensitivity analysis. The influence tendency and significance for each input parameter were described by the calculation of sensitivity coefficient (S_x) [23]. The

Table 2. Interval values of the major physicochemical properties for 16 PAHs (25°C).[a]

PAHs	Abbr.	T_M(°C)	S_W(mg L^{-1})	P_S(Pa)	log K_{OW}	H_F (h)			
						Air	Water	Soil	Sediment
Naphthalene	NAP	[80.0, 80.5]	$[3.10 \times 10^{1}, 3.17 \times 10^{1}]$	$[1.10 \times 10^{1}, 1.13 \times 10^{1}]$	[3.30, 3.50]	[17.00, 18.00]	[170, 912]	[1700, 1800]	[5500, 8160]
Acenaphthyene	ANY	[92.0, 124.0]	$[3.93 \times 10^{0}, 1.60 \times 10^{1}]$	$[8.90 \times 10^{-1}, 8.93 \times 10^{-1}]$	[3.94, 4.07]	[0.91, 5.00]	[360, 550]	[550, 720]	[3600, 5500]
Acenaphthlene	ANA	[93.0, 108.0]	$[1.93 \times 10^{0}, 3.90 \times 10^{0}]$	$[2.90 \times 10^{-1}, 2.93 \times 10^{-1}]$	[3.92, 3.98]	[5.00, 5.76]	[550, 912]	[1700, 1800]	[5500, 8160]
Fluorene	FLU	[110.0, 119.0]	$[1.68 \times 10^{0}, 1.98 \times 10^{0}]$	$[7.80 \times 10^{-2}, 8.00 \times 10^{-2}]$	[4.18, 4.18]	[17.00, 43.20]	[360, 550]	[550, 720]	[3360, 5500]
Phenanthrene	PHE	[99.0, 136.0]	$[1.15 \times 10^{0}, 1.20 \times 10^{0}]$	$[1.60 \times 10^{-2}, 2.50 \times 10^{-2}]$	[4.45, 4.57]	[28.80, 55.00]	[550, 1440]	[2880, 5500]	[12960, 17000]
Anthracene	ANT	[136.0, 220.0]	$[4.30 \times 10^{-2}, 7.60 \times 10^{-2}]$	$[8.67 \times 10^{-4}, 1.10 \times 10^{-3}]$	[4.45, 4.54]	[9.60, 55.00]	[550, 1440]	[2880, 5500]	[12960, 17000]
Fluoranthene	FLT	[110.0, 166.0]	$[2.00 \times 10^{-1}, 2.60 \times 10^{-1}]$	$[1.10 \times 10^{-3}, 1.23 \times 10^{-3}]$	[4.90, 5.22]	[12.96, 55.00]	[1440, 1700]	[1700, 2880]	[12960, 17000]
Pyrene	PYR	[150.0, 166.0]	$[1.30 \times 10^{-1}, 1.32 \times 10^{-1}]$	$[5.50 \times 10^{-4}, 6.00 \times 10^{-4}]$	[4.88, 5.18]	[5.00, 7.68]	[1440, 1700]	[1700, 2880]	[12960, 17000]
Benzo [a] anthracene	BaA	[84.0, 177.0]	$[9.00 \times 10^{-3}, 1.00 \times 10^{-2}]$	$[1.50 \times 10^{-5}, 2.80 \times 10^{-5}]$	[5.61, 5.91]	[5.00, 7.68]	[1440, 1700]	[1700, 2880]	[12960, 17000]
Chrysene	CHR	[170.0, 260.0]	$[2.00 \times 10^{-3}, 2.80 \times 10^{-3}]$	$[6.10 \times 10^{-7}, 8.27 \times 10^{-7}]$	[5.16, 5.86]	[5.00, 7.68]	[1440, 1700]	[1700, 2880]	[12960, 17000]
Benzo [b] fluoranthene	BbF	[168.0, 209.0]	$[1.50 \times 10^{-3}, 1.20 \times 10^{-2}]$	$[2.10 \times 10^{-5}, 6.67 \times 10^{-5}]$	[5.78, 6.04]	[17.00, 21.12]	[1440, 1700]	[1700, 2880]	[12960, 17000]
Benzo [k] fluoranthene	BkF	[194.0, 220.0]	$[7.60 \times 10^{-4}, 8.00 \times 10^{-4}]$	$[1.29 \times 10^{-7}, 1.30 \times 10^{-7}]$	[6.04, 6.11]	[5.00, 7.20]	[1440, 1700]	[1700, 2880]	[12960, 17000]
Benzo[a] pyrene	BaP	[179.0, 209.0]	$[1.60 \times 10^{-3}, 4.00 \times 10^{-3}]$	$[7.33 \times 10^{-7}, 7.50 \times 10^{-7}]$	[6.06, 6.13]	[5.00, 7.68]	[1440, 1700]	[1700, 2880]	[12960, 17000]
Indeno[1, 2, 3-cd] pyrene	IPY	[160.0, 233.0]	$[2.60 \times 10^{-7}, 5.00 \times 10^{-4}]$	$[1.00 \times 10^{-10}, 1.73 \times 10^{-8}]$	[6.69, 6.84]	[5.00, 6.00]	[1440, 1700]	[1700, 2880]	[12960, 17000]
Dibenz [a, h] anthracene	DBA	[218.0, 270.0]	$[6.00 \times 10^{-4}, 2.50 \times 10^{-3}]$	$[4.30 \times 10^{-10}, 1.27 \times 10^{-7}]$	[6.50, 6.84]	[5.00, 7.68]	[1440, 1700]	[1700, 2880]	[12960, 17000]
Benzo [ghi]perylene	BPE	[218.0, 280.0]	$[2.60 \times 10^{-4}, 6.20 \times 10^{-4}]$	$[1.33 \times 10^{-8}, 1.40 \times 10^{-8}]$	[6.50, 6.63]	[4.32, 5.00]	[1440, 1700]	[1700, 2880]	[12960, 17000]

[a] M_W is molecular weight; T_M is melting point; S_W is water solubility; P_S is vapour pressure; log K_{ow} is octanol–water partition coefficient in logarithmic units; and H_F is estimated half-life periods in the multimedia environments.

The physicochemical properties values were obtained from the interval values of literature [15] and [19].

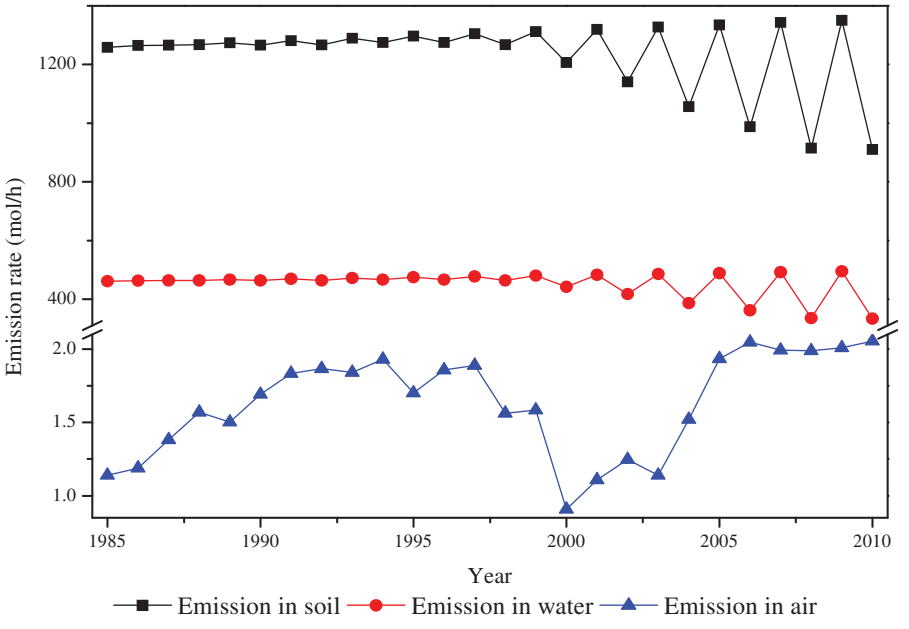

Figure 1. Average emission rates of ∑16 PAHs in different compartments from 1985 to 2010.

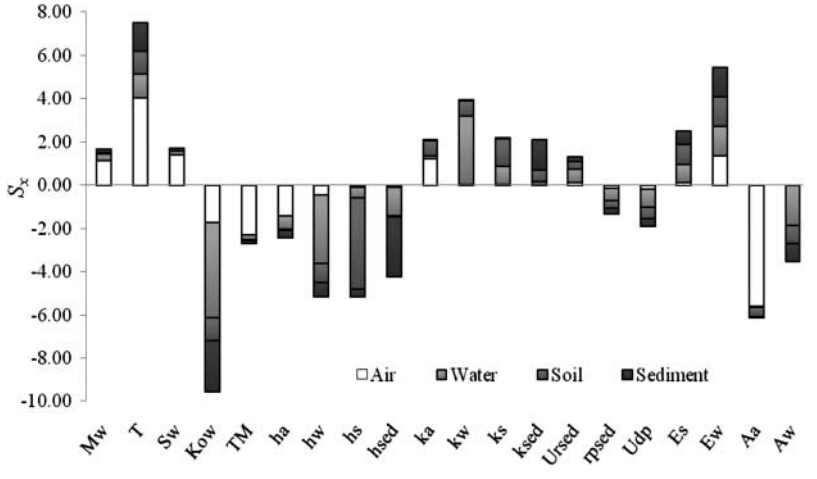

Figure 2. Sensitivity coefficients of the key parameters in various compartments.

calculation results of the sensitivity coefficients for key parameters (the sum of the S_x in different compartments is higher than 1.0) are shown in Figure 2.

From the calculation results of S_x, all of the input parameters were divided into three categories. In the first category, the modelling results were increased by the increase in the individual input, such as the molecular weight (M_w), environmental temperature (T), water solubility (S_w), degradation rate (k_a, k_w, k_s, and k_{sed}), suspended particles and water partition coefficient (U_{rsed}), and source emissions in different compartments (E_s and E_w). In the second category, themodelling results were decreased by the increase in the individual input, for instance, K_{OW}, vapour pressure (T_M), the suspended solid density (rp_{sed}), sediment deposition rate (U_{dp}), and the depths (h_a, h_w, h_s, and h_{sed}) and areas (A_a and A_w) of the bulk compartment. In the third category, it

was determined that the input parameters, such as Henry's constant, air–side and air–water diffusion, rain dissolution to water, and scavenging rate, had no significant influence on the modelling results. When the absolute value of S_x was used to indicate the significance of each parameter, it was found that the environmental temperature, Kow, and depths and areas of the bulk compartment were the most sensitive parameters for adjusting the model uncertainty.

3.2. *Validation of the interval solutions*

Compare the modelled and observed concentrations of the pollutants. Because of huge regional-ties the acceptable difference between two values should be less than one logarithm unit. The observed concentrations mainly come from literature, experiment, or data of adjacent district have similar properties to those of the study area [24]. The data used to validate the model reliability in soil and water were obtained from the actual experiment [25]. PAH concentrations in air and sediment compartments were obtained from the literature data of adjacent district and the study area, respectively [26,27].

Comparisons between the measured concentrations and the modelled ones in this study are shown in Table 3.

The IALREs of the IDMF model were calculated as 0.41, 0.63, 0.52, and 0.58 for the air, water, soil, and sediment compartments, respectively, which showed good agreement between the modelled values and the measured ones. Some simulation results were underestimated, which could be explained by the serious pollution situation in the sampling area and the unquantified additional sources [28]. PAHs in water and sediment were sampled near the oil exploitation area, in which there were hundreds of chemical plants, steel rolling mills, sulfuric acid plants, paper mills. Meanwhile, soil samples used to validate the model reliability were collected around six oil wells, in which oil spilled on soil could be observed in some places.

The IDMF modelled PAH concentrations were similar to the modelled results applying a certainty fugacity model to a similar ecosystem [16], and the IDMF modelled IALREs were less than the certainty ALREs (0.45–0.79). Besides, the accurate numerical range of the simulated concentrations could be described by the developed IDMF model. Owing to the complexity of the researched environmental system, the measured concentrations may vary by several orders of magnitude, and the validation between the deterministic solution and the measured value with standard deviations may lack reliability in the current conditions.

3.3. *Uncertainty analysis*

Uncertainty of the IDMF model was directly indicated by the interval presentation. The dynamic results of the interval simulation for PAHs in the four bulk compartments are shown in Figure 3, which reveals that the dispersions of the concentrations for each compartment were large and generally covered one to two orders of magnitude. The average coefficients of variation (CV) of the simulated concentrations in air, water, soil, and sediment compartments were 0.36, 2.94, 2.31, and 1.06, respectively. Compared to the model CV, the CV of the measured concentration was

Table 3. Validation results between the measured values and the modelled ones.

Compartments (Unit)	Lower bound		Upper bound		ALREl	ALREu	IALRE
	Measured	Modelled	Measured	Modelled			
Air (gm^{-3})	1.30×10^{-4}	4.10×10^{-5}	3.21×10^{-4}	6.70×10^{-4}	0.50	0.32	0.41
Water (μgL^{-1})	3.46×10^{-1}	8.79×10^{-2}	4.09×10^{1}	8.69×10^{0}	0.60	0.67	0.63
Soil ($ng\,g^{-1}$)	2.18×10^{2}	1.36×10^{2}	4.58×10^{4}	6.62×10^{3}	0.21	0.84	0.52
Sediment ($ng\,g^{-1}$)	4.87×10^{1}	5.41×10^{0}	4.06×10^{2}	6.53×10^{2}	0.95	0.21	0.58

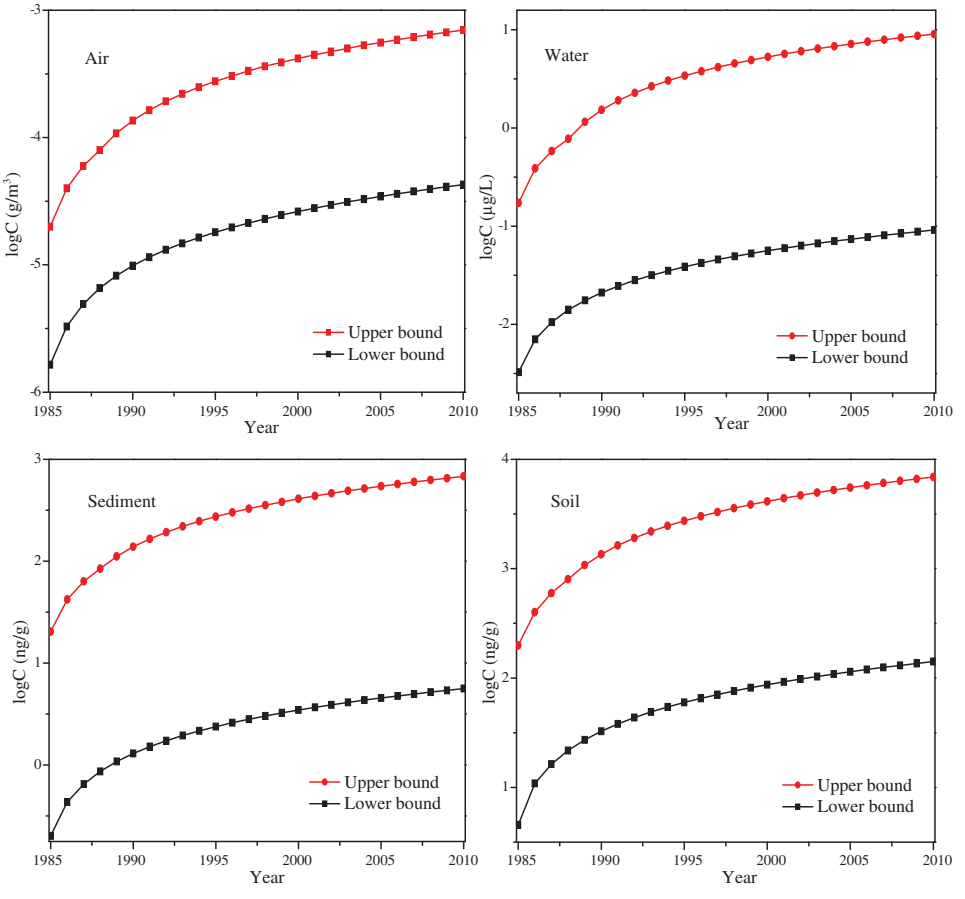

Figure 3. Dispersions of PAHs concentrations in different compartments during 1985–2010 derived from interval solution.

calculated as 1.06 for water, 3.79 for soil, and 1.10 for sediment; the measured concentration for the air compartment lacked sufficient test results. Soil compartments had the largest uncertainty owing to the complexity of the environmental system. The modelled CV in the water is much larger than the measured one because of the measured values are less variable than the modelled values, this may be produced by the underestimations of lower and upper bounds of the modelled values. For example, the CV would be higher with the lower average value under the same deviation. In conclusion, the uncertainty of the IDMF model was comparable to the variability of the measured concentration.

The use of interval arithmetic resulted in comparable uncertainty to other methods. Some advantages could be found in the combination of the traditional fugacity model with interval arithmetic. First, the input parameters of the model were easily obtained compared with other random and fuzzy uncertainty methods, as only upper and lower bound input parameter values are needed [29]. Second, the interval arithmetic was relatively simple and could be solved by the Euler method, and the uncertainties of the model could be expressed as the upper and lower bounds [30].

3.4. *Dynamic multimedia environmental fate*

Temporal trends in the total concentrations of the 16 PAHs in air (gm^{-3}), water (μgL^{-1}), soil (ngg^{-1}), and sediment (ngg^{-1}) from 1985 to 2010 were simulated by the IDMF model.

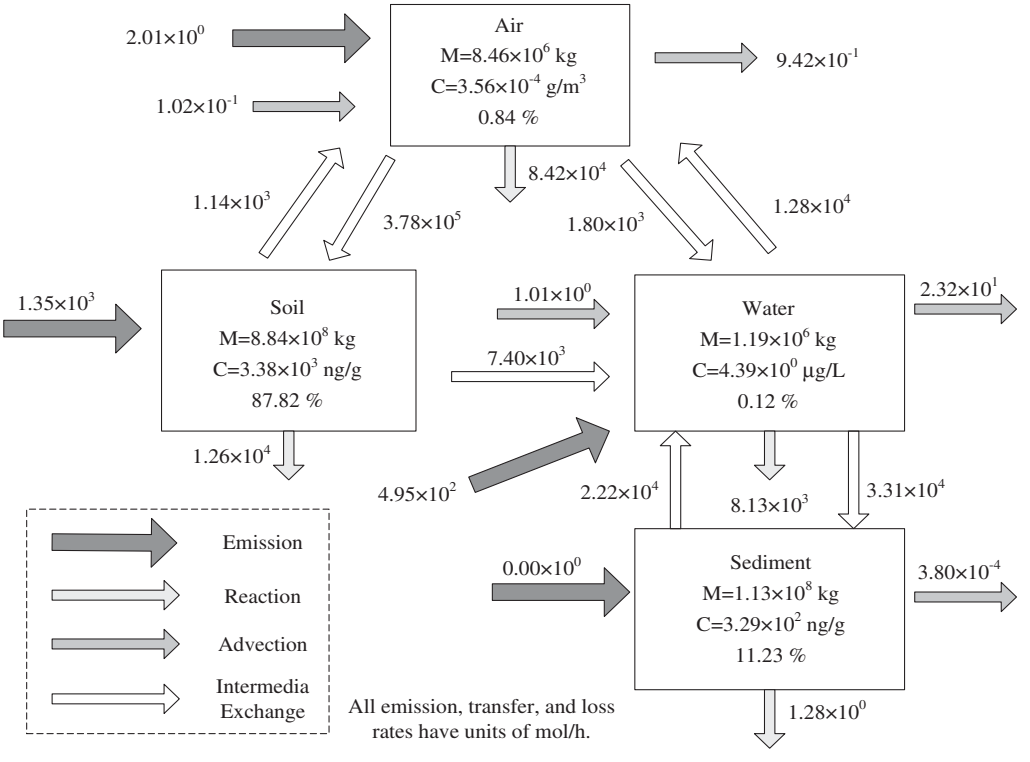

Figure 4. Environmental process rates of ∑16 PAHs in multimedia environment in 2010.
Note: The environmental process (emission, reaction, advection, and intermedia exchange) rates were expressed by different types of arrow, and the environmental fates (masses, concentrations, and distribution percentages) of PAHs in the multimedia environments were shown in the boxes.

The concentrations showed an overall increasing trend from 1985 to 2010. The PAH concentrations were increased to 29.55 times the values in air, 39.22 times the values in water, 31.98 times the values in soil, and 26.69 times the values in sediment. These increases revealed an obvious cumulative effect in the multimedia environment, which could be explained by the calculation results of the major environmental process rates for ∑16 PAHs in 2010 (Figure 4). Because of the principle of mass conservation, if the total speed of pollutant inputs into a compartment (emission, inflows, and intermedia exchange) is faster than the total speed of pollutant outputs from the compartment (reaction, outflow, and intermedia exchange), there must be an accumulative effect in the compartment. In the study area, the cumulative effect of PAHs must be caused by the large-scale, high-intensity, and long duration of petroleum extraction, and PAHs entered into air, water, and soil compartments through pathways of hydrocarbon volitilisation, oilfield wastewater discharge, and oil spills on soil.

The transfer and distribution of PAHs were evaluated based upon the percent that each environmental process occupied. The soil source emission (65.24%), and source emission in water (34.54%) was identified as the major PAH sources to this oilfield. Degradation in air (80.22%) and degradation in soil (12.01%) were the major outputs. The dominant transfer process in the study area was dry/wet deposition from air to soil (82.81%). The simulation results of PAHs environmental behaviors were in accordance with the intermedia exchange investigation that air-to-soil exchange was the most remarkable among all of the environmental processes assumed in the model [31,32].

The maximum amount of PAHs in the environment occurred in 2010. Soil was the dominant sink, accounting for 87.35% in 1985 and 87.82% in 2010. The PAH fractions in air, water, and sediment were 0.87%, 0.05%, and 11.75%, respectively, of the total amount in 1985 and 0.84%, 0.12%, and 11.23%, respectively, of that in 2010. The simulation results of PAHs distribution in the multimedia environments were consistent with the previous studies of PAHs partitioning in natural environment [33,34].

Through the IDMF model developed in this study, the PAHs concentrations in the multimedia environments were derived. These results could be used for ecological risk assessment (ERA) of PAHs in the typical oilfield. The proposed multimedia fugacity model could serve as a fundamental for developing an effect model and fate-transport-effect (FTE) model to solve ecotoxicological problems and perform ERA of PAHs in the typical oilfield. Further, the combination of interval parameter and stochastic simulation would aid in presenting the uncertainties inherent in ERA.

3.5. *Dynamic source apportionment*

The relative abundances or diagnostic ratios are useful indicators of PAH sources because isomer pairs are diluted to a similar extent upon mixing with natural particulate matter; additionally, they are distributed similarly to other phases because they have comparable thermodynamic partitioning and kinetic mass transfer coefficients [2]. The pathways of PAHs entering the environment are primarily divided into three processes: petroleum release, high-temperature combustion of organic compounds, and biomass and coal combustion [35]. Diagnostic ratios of PAHs, such as the ratio of IPY/(IPY + BPE), could be used to identify the possible emission sources. It was reported that IPY/(IPY + BPE) < 0.2 was characteristic of petroleum sources, $0.2 <$ IPY/(IPY + BPE) < 0.5 was characteristic of high-temperature combustion origin, and IPY/(IPY + BPE) > 0.5 was characteristic of biomass and coal combustion [36,37]. To identify the PAH sources in the oilfield, ratios of IPY/(IPY + BPE) based on the dynamic interval simulation are presented in Figure 5.

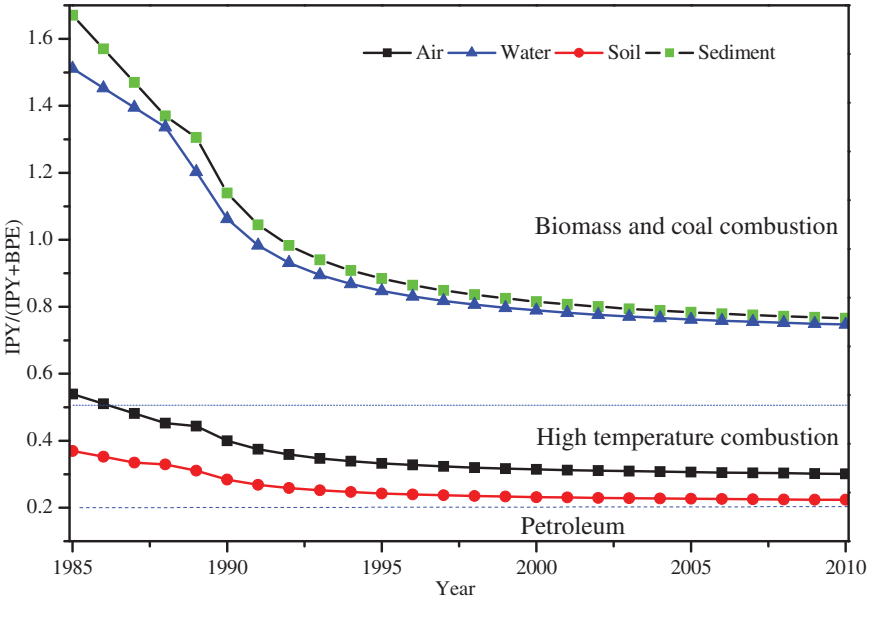

Figure 5. Dynamic ratios of IPY/(IPY+BPE) in the multimedia environments.

From Figure 5, it can be observed that the ratios of IPY/(IPY + BPE) ranged from 0.2 to nearly 1.7. Specifically, the ratios from 1986 to 2010 were between 0.2 and 0.6 in the air compartments, whereas those were 0.2 to 0.4 in the soil compartment. The results show that PAHs in the air and soil compartments primarily come from high-temperature combustion of organic compounds, which was derived from biomass and coal combustion in the air during 1985–1986. Meanwhile, the ratios of IPY/(IPY + BPE) in the water and sediment compartments were from 0.7 to 1.7; these were similar to measures for biomass and coal combustion. The ratio of IPY/(IPY + BPE) in the multimedia environments showed an overall decreasing trend, which tended to be from petroleum sources as evidenced by the accumulation effect of PAHs and continuous oil exploitation. The ratio of IPY/(IPY + BPE) in the soil compartment was the closest to the petroleum origin because oil spills on soil was direct source emission in the soil compartment. Therefore, high-temperature combustion was the major source of PAHs in air and soil, whereas biomass and coal combustions were attributed to water and sediment.

4. Conclusions

The concentrations of Σ16 PAHs in the four compartments were increased by almost 30 times in 2010. Based on the model calculations, the leading environmental behaviour was atmospheric deposition from air to soil, and the major sink was the soil compartment by the model calculations. Dynamic source apportionment indicated that high-temperature combustion was the major source of PAHs in the air and soil compartments, whereas biomass and coal combustion were the primary contributors to water and sediment PAHs during the study period.

Acknowledgements

This study was supported by the Key Projects in the National Science & Technology Pillar Program in the Eleventh Five-Year Plan Period (2008BAC43B01), and we thank the Elsevier Language Editing Services for the editorial revisions.

References

[1] Luch A. The carcinogenic effects of polycyclic aromatic hydrocarbons. London: Imperial College Press; 2005.
[2] Wang DG, Yang M, Jia HL, Zhou L, Li YF. Polycyclic aromatic hydrocarbons in urban street dust and surface soil: comparisons of concentration, profile, and source. Arch. Environ. Con. Tox. 2009;56:173–180.
[3] Liu Y, Chen L, Huang QH, Li WY, Tang YJ, Zhao JF. Source apportionment of polycyclic aromatic hydrocarbons (PAHs) in surface sediments of the Huangpu River, Shanghai, China. Sci. Total Environ. 2009;407:2931–2938.
[4] CNBS (China's National Bureau of Statistics). China energy statistic yearbook 2007. Beijing: China Statistical Press; 2008.
[5] Qiu HG, Huang JK, Yang J, Rozelle S, Zhang YH, Zhang YL. Bioethanol development in China and the potential impacts on its agricultural economy. Appl. Energ. 2010;87:76–83.
[6] Grec A, Maior C. Earth oil extraction-major environmental pollution source. Environ. Eng. Manag. J. 2008;7:763–768.
[7] Wang R, Cao HY, Li W, Wang W, Wang WT, Zhang LW, Liu JM, Ouyang HL, Tao S. Spatial and seasonal variations of polycyclic aromatic hydrocarbons in Haihe Plain, China. Environ. Pollut. 2011;159:1413–1418.
[8] Ao JT, Chen JW, Tian FL, Cai XY. Application of a level IV fugacity model to simulate the long-term fate of hexachlorocyclohexane isomers in the lower reach of Yellow River basin. China. Chemosphere 2009;74:370–376.
[9] Moore RE. Interval analysis. New York: Prentice-Hall; 1966.
[10] Moore RE, Kearfott RB, Cloud MJ. Application of interval analysis. Philadelphia: Society for Industrial and Applied Mathematics; 2009.
[11] Li G, Xia X, Yang Z, Wang R, Voulvoulis N. Distribution and sources of polycyclic aromatic hydrocarbons in the middle and lower reaches of the Yellow River, China. Environ. Pollut. 2006;144:985–993.
[12] Wang XC, Sun S, Ma HQ, Liu Y. Sources and distribution of aliphatic and polyaromatic hydrocarbons in sediments of Jiaozhou Bay, Qingdao, China. Mar. Pollut. Bull. 2006;52:129–138.
[13] Yunker MB, Macdonald RW, Vingarzan R, Mitchell H, Goyette D, Sylvestre S. PAHs in the Fraser River basin: a critical appraisal of PAHs ratios as indicators of PAH source and composition. Org. Geochem. 2002;33:489–515.
[14] Morillo E, Romero AS, Madrid L, Villaverde J, Maqueda C. Characterization and sources of PAHs and potentially toxic metals in urban environments of sevilla (Southern Spain). Water Air Soil Poll. 2008;187:41–51.

[15] Mackay D. Multimedia environmental models: the fugacity approach. New York: Lewis Publishers; 1991.
[16] Li Y, Hu Y, Du XY, Wang Y. Investigation on the dynamic environmental behaviors of petroleum-derived polycyclic aromatic hydrocarbons in an oilfield, China. Fresen. Environ. Bull. 2012;21:986–994.
[17] Cao HY, Liang T, Tao S, Zhang CS. Simulating the temporal changes of OCP pollution in Hangzhou, China. Chemosphere 2007;67:1335–1345.
[18] Mackay D, Paterson S. Evaluating the multimedia fate of organic chemicals: a level III fugacity model. Environ. Sci. Technol. 1991;25:4227–436.
[19] Profiler PBT, *Persistent, bioaccumulative, and toxic profiles estimated for organic chemicals*. 2012. Available from: http://www.pbtprofiler.net.
[20] Xu SS, Liu WX, Tao S. Emission of polycyclic aromatic hydrocarbons in China. Environ. Sci. Technol. 2006;40:702–708.
[21] Zhang HY. Study on the distribution of BTEX and PAHs in refinery wastewater and environmental risk assessment [master dissertation]. Shandong: Shandong University; 2008.
[22] Chen JJ, Wang HQ, Xi CG, Zhang J. Environmental impact of oil pollutant on groundwater during oilfield exploitation in Daqing-a modelling analysis. Chinese J. Appl. Ecol. 2001;12:113–116.
[23] Mongan MG, Henrion M. Uncertainty – a guide to dealing with uncertainty in quantitative risk and policy analysis. Cambridge: Cambridge University Press; 1990.
[24] Li YF, Cao HY. Prospects for future application of fugacity model to fate studying of POPs in China. Wuhan Univ. J. Natural Sci. 2003;8:996–1000.
[25] Li Y, Hu Y, Du XY, Liu JL. The contributions of polycyclic aromatic hydrocarbons to soil biotoxicity. Energy Sources, Part A: Recovery, Utilization, Environm. Effects, accepted for publication, doi:10.1080/15567036.2011.603024.
[26] Hong Y, Piao FY, Wang YY, Liu S, Liu P. Concentrations and distributions of ambient particulate matter and polycyclic aromatic hydrocarbons in an industrial city of northeastern China. Chinese Med. J. Metall. Ind. 2008;3:278–279.
[27] Liu GM, Yin LL, Liu ZJ, Xue JL. Distributional characteristics of polycyclic aromatic hydrocarbons in vertical section of sediments from Zhalong wetland. Res. Environ. Sciences 2008;21:36–39.
[28] Mackay D, Hickie B. Mass balance model of source apportionment, transport and fate of PAHs in Lac Saint Louis, Quebec. Chemosphere 2000;41:681–692.
[29] Huang GH, Morre RD. Grey linear programming, its solving approach, and its application. Int. J. Systems Sci. 1993;24:159–172.
[30] Zhang H. Nondeterministic linear static finite element analysis: an interval approach [Ph.D. dissertation]. Georgia Institute of Technology; 2005.
[31] Wang R, Cao HY, Li W, Wang W, Wang WT, Zhang LW, Liu JM, Ouyang HL, Tao S. Spatial and seasonal variations of polycyclic aromatic hydrocarbons in Haihe Plain, China. Environ. Pollut. 2011;159:1413–1418.
[32] Ni HG, Qin PH, Cao SP, Zeng H. Fate estimation of polycyclic aromatic hydrocarbons in soils in a rapid urbanization region, Shenzhen of China. J. Environ. Monit. 2011;13:313–318.
[33] Wild SR, Jones KC. Polynuclear aromatic hydrocarbons in the United Kingdom environment: a preliminary source inventory and budget. Environ. Pollut. 1995;88:91–108.
[34] Maliszewska-Kordybach B. Sources, concentrations, fate and effects of polycyclic aromatic hydrocarbons (PAHs) in the environment. Part A: PAHs in air. Pol. J. Environ. Stud. 1999;8:131–136.
[35] Neff JM. Polycyclic aromatic hydrocarbons in the aquatic environment sources fates and biological effects. London: Applied Science; 1979.
[36] Soclo HH, Garrigues PH, Ewald M. Origin of polycyclic aromatic hydrocarbons (PAHs) in coastal marine sediments: case studies in Cotonou (Benin) and Aquitaine (France) areas. Mar. Pollut. Bull. 2000;40:387–396.
[37] Baumard P, Budzinski H, Garrigues P. Polycyclic aromatic hydrocarbons in sediments and mussels of the western Mediterranean Sea. Environ. Toxicol. Chem. 1998;17:765–776.